JOURNAL OF MATERIALS SCIENCE **39** (2004) 2509–2515

# Influence of alumina content on the nucleation crystallization and microstructure of barium fluorphlogopite glass-ceramics based on $8SiO_2 \cdot yAl_2O_3 \cdot 4MgO \cdot 2MgF_2 \cdot BaO$

## Part II *Microstructure, microhardness and machinability*

J. HENRY
*Department of Material Science and Technology, University of Limerick, Plassey Park, Limerick, Ireland*

R. G. HILL
*Department of Materials, Imperial College of Science, Technology and Medicine, London SW7 2BP, UK*
*E-mail: r.hill@ic.ac.uk*

The influence of alumina content, heat treatment time and temperature on the microstructure, hardness and theoretical machinability of barium fluorphlogopite glass-ceramics were investigated. The glass-ceramics were based on glasses of the general composition $8SiO_2$-$yAl_2O_3$-3.75MgO-2.25$MgF_2$-BaO. Glasses with high alumina contents with $y > 2.0$ were found to give fine feathery microstructures that did not coarsen readily to give the classic house of cards microstructure associated with machinability. The glass with the lowest alumina content ($y = 1.5$) that gave a house of cards microstructure was therefore investigated in detail. The Vickers hardness decreased slightly on formation of the barium fluorphlogopite phase, but decreased significantly on forming an interconnected house of cards microstructure. Machinability was highly dependent on the formation of an interconnected microstructure. 

### 1. Introduction

Mica glass-ceramics are commercially important machinable ceramics that can be cut and turned without using diamond tipped tooling. They are used widely in the optoelectronics area and for production of scientific equipment. They are particularly attractive compared to metals where thermal or electrical insulation is required. However, the strength and fracture toughness of the commercial materials such as Macor$^{TM}$ are relatively poor for many applications.

Recently it has been shown that if the potassium is replaced by barium in fluormica glass-ceramics then much higher strength and fracture toughness values can be obtained as well as improved machineability [1]. The barium ions replace the potassium ions in the layers between the mica planes and make cleavage along the 100 direction more difficult.

The nucleation and crystallization behaviour of fluormica glass-ceramics was reported in Part I [2].

#### 1.1. Machinability

Machinability is a property of a material that describes the ease or the difficulty involved in machining a component with a cutting tool [3]. In terms of trying to quantify the machining operation, factors such as tool wear, tool life, cutting energy involved in the material removal process, forces expended on the cutting tooland the quality or topography of the machined surface have been used in the determination of the machinability of a variety of metals and glass-ceramics. In this case, the term 'machinability' is assessed by the manufacturing process and machined material characteristics after trying to shape a material. This gives a realistic value by which to grade different materials in a range of machining operations. The shaping of mica glass-ceramics generally combines machining and grinding processes, which are associated with the crystal and residual glass phase powder produced from the machining operation, which is highly abrasive.

#### 1.2. Determination of machinability

Grossman [4] investigated the machinability of a tetrasilicic fluormica glass-ceramic by examining the amount of time required to drill through a standard thickness. The results of this analysis showed that machinability increases with decreasing strength. The reasons for this are based on microstructural variables, such as the volume fraction of fluormica crystals, the

aspect ratio, crystal size and the degree of crystal connectivity in the microstructures formed [4]. Grossman suggested that glass-ceramics containing as little as $\frac{1}{3}$ by volume of mica crystals might be machinable if the aspect ratio of the crystals is high enough to cause a high degree of crystal connectivity. In fine-grained fluormica glass-ceramics with an average crystal size smaller than 4.5 $\mu$m, an increase in strength is proportional to the $\frac{1}{5}$ power of the average mica-plate diameter. In this type of microstructure, fracture could propagate freely through the glass matrix, and therefore crack arrestment would be poor. Larger crystals with higher aspect ratios would be able to hinder fracture by blunting cracks through an interconnected crystal microstructure. This form of microstructure was obtained when the crystal size exceeded 4.5 $\mu$m. The strength was then inversely proportional to the first power of the mica plate diameter. Unfortunately, the ease of machining is also inversely proportional to the mechanical strength.

Grossman [5] also provided a method for obtaining the machinability index (MI) from an in-house mechanical hacksaw apparatus. The machinability index is calculated from the following expression:

$$\mathrm{MI} = \frac{S}{1/2W(T_1 + T_2)10}$$

where $S$ is the number of strokes (20), $W$ is the width of the sample and $T_1$ and $T_2$ are the depths of each end of cut. However, this method gives only a rough measure of the stock removal rates because the hacksaw is a general cutting instrument. Other factors, such as the measurement of the depth of cut, make this procedure difficult to use and the actual forces exerted during the machining operation cannot be obtained.

Evans and Marshall carried out the first work on investigating the fundamental processes involved in machining glass-ceramics [6]. Indentation fracture mechanics was used as a method of investigating the material removal rate during a grinding operation. Evans and Marshall concluded that there were two modes of material removal: crushing and lateral cracking, which were sensitive to the load applied. However, since this research, there is strong experimental evidence that material removal processes occur by a cleavage fracture process [7].

Baik *et al.* carried out an in depth study into the evaluation of machinability. They concluded that the microhardness of a material controls the machining characteristics of fluormica glass-ceramics [8]. Further work by Baik *et al.* investigated a relationship between microstructural parameters such as crystal aspect ratio, percentage crystallinity and interconnectivity, with machinability [9]. An interconnected crystal microstructure is required to deflect and blunt the propagation of cracks formed during a shaping process. A higher degree of crystal connectivity (higher effective crystallinity) leads to a reduction in the microhardness. When the microhardness data are plotted against the effective crystallinity data, an inflection point in the curve describes the optimum microstructure, which should be highly machinable. The approach used by Baik *et al.* is used in the present paper and is covered in more detail in the experimental section.

Finally, Boccaccini [10] developed further the work of Baik *et al.* and produced an evaluation of machinability based on a correlation between brittleness and machinability. Machinability information was developed from the slope of a log-log plot of specific cutting energy against cutting rate for a range of different machinable glass-ceramics. This research developed a brittleness factor ($B$) which relates hardness ($H_\mathrm{v}$) and fracture toughness ($K_{1\mathrm{C}}$) through the equation:

$$B = \frac{H_\mathrm{v}}{K_{1\mathrm{C}}}$$

The intention was to apply this approach in the present study using an indentation fracture test to determine fracture toughness. However, it proved impossible to obtain valid measurements because of crack deflection of the indentation cracks.

## 2. Experimental

### 2.1. Glass synthesis

The synthesis of the glasses has been described in Part I [2]. Monolithic glass samples were prepared by remelting the glass frits produced in Part I in alumina crucibles and casting the resulting melt into graphite crucibles held at the glass transition temperature—50 K.

The glasses were based on the following generic series $8SiO_2{\cdot}yAl_2O_3{\cdot}4MgO{\cdot}2MgF_2{\cdot}BaO$ for which the alumina content was varied between $1.5 \leq y \leq 3$.

### 2.2. Microstructural analysis

Samples for the investigation of microstructural development were all held for one hour at the previously determined optimum nucleation temperature followed by heating at 10°C min$^{-1}$ to the given crystal growth temperature. The $y = 1.5$ glass was selected for a detailed study of the influence of heat treatment time and temperature on the microstructure, volume fraction of the fluorphlogopite phase formed and the hardness. This glass was selected because the only crystalline phase to form was barium fluorphlogopite and a classic house of cards microstructure was formed.

Four crystallization temperatures (Tc) were chosen:

1150°C = Tc1 with 1, 4, 8 and 16 hour isothermal holds.

1175°C = Tc2 with 1, 4, 8 and 16 hour isothermal holds.

1190°C = Tc3 with 1, 4 and 8 hour isothermal holds.

1200°C = Tc4 with 1 and 4 hour isothermal holds.

Samples of glass were embedded in epoxy resin and polished to an optical finish using 1 $\mu$m diamond paste. Samples were then examined by scanning electron

microscopy in the back scattered and secondary electron imaging modes.

### 2.3. Microhardness analysis

Microhardness analysis was conducted on the SEM samples embedded in epoxy resin using a LECO Microhardness indenter, M400-G1 (LECO Ltd., Japan). A load ($P$) of up to 500 g was used in conjunction with a Vickers diamond indenter (face angle 136°) for 15 s in accordance with ASTM standard E 384-89 [11]. The indentation was measured using Buehler Imaging software (Enterprise Software, Buehler, USA). The Vickers hardness number, $H_v$, was calculated using the following expression:

$$H_v = \frac{1.8544\,P}{d^2}$$

where $H_v$ is the Vickers Hardness (GPa), $P$ is the applied load (kg) and $d$ is the mean of the lengths of the diagonals of the indentation (mm).

### 2.4. Determination of machinability

A number of parameters first determined by Baik *et al.* [8, 9] were calculated from the hardness data and microstructural parameters. These include $u_1$ the cutting energy at the quasi-static state given by:

$$u_1 = H_v^{2.25}$$

The machinability parameter, $n$, can also be used to categorise the effects of various heat treatments as a function of temperature, time and $H_v$. The following equation indicates the relationship between hardness ($H_v$) and machinability.

$$n = 0.643 - 0.122 H_v$$

Finally, Baik *et al.* [8, 9] also defined a parameter termed the Effective Crystallinity parameter, $Xe$, was determined. Using the expressions:

$$Xe = 1 - \exp(M \ln(1 - x))$$

$$M = \left[\frac{(A)^{2/3} + 2(A)^{-1/3}}{3}\right]^{3/2}$$

where $M$ is a multiplication factor related to the connectivity of a disk-like crystal, $A$ is the average aspect ratio and $x$ is the actual volume fraction that has crystallised. The volume fraction crystallinity is replaced by the area fraction calculated using imaging analysis. This analysis can deduce the variation of crystal connectivity and its resultant effects on the microhardness values obtained.

The approach pursued here is specific to mica glass-ceramics in which the crack propagates in either a transgranular or an intergranular manner. This is associated with a weak crystal/glass interface or interlayer crystal bonding. A high degree of crystal connectivity is observed which results in a machinable glass-ceramic. The interconnected crystal network blunts fracture paths and thus prevents catastrophic failure of a sample during machining. These glass-ceramics are known to have low microhardness values. Hence, microhardness analysis can be utilised to investigate the machinability by analysing how various fluormica crystal microstructures respond to deformation. The reason for this is that the microhardness analysis mimics the material removal rate during machining. The various heat treatments applied will pinpoint the best crystal distribution and microstructure by investigating the ability of a sample to tolerate indentation.

## 3. Results and discussion

Figs 1 and 2 show typical microstructures formed for the glasses with high alumina contents. Glasses with high alumina contents gave microstructures with a leaf like appearance that did not coarsen readily. The glasses with high $y$ values have excess alumina over that required to form the barium fluorphlogopite phase. Consequently a large amount of alumina is left in the residual glass phase and crystallization of barium fluorphlogopite is inhibited and crystal growth restricted by the high viscosity of this residual glass phase.

When the alumina content is reduced the mica crystals can coarsen and grow. In the lowest alumina content

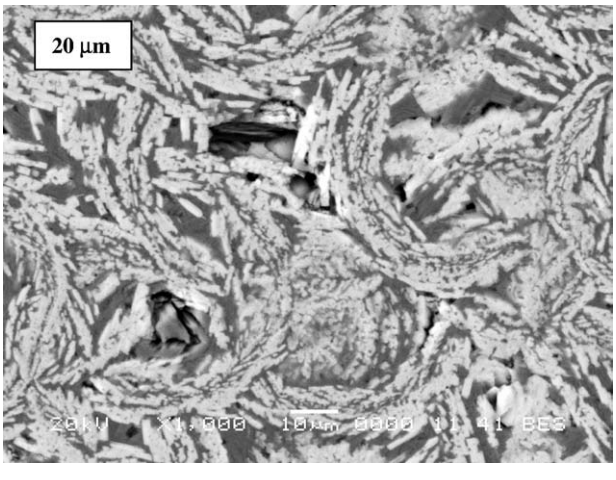


*Figure 1* Microstructure of $y = 2.00$ glass heat treated at 655°C for 1 h and at 1000°C for 5 h.

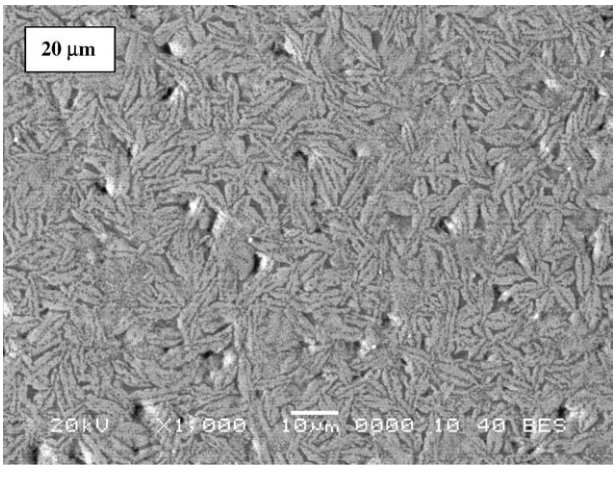


*Figure 2* Microstructure of $y = 3$ glass heat treated at 685°C for 1 h and at 965°C for 2.5 h.

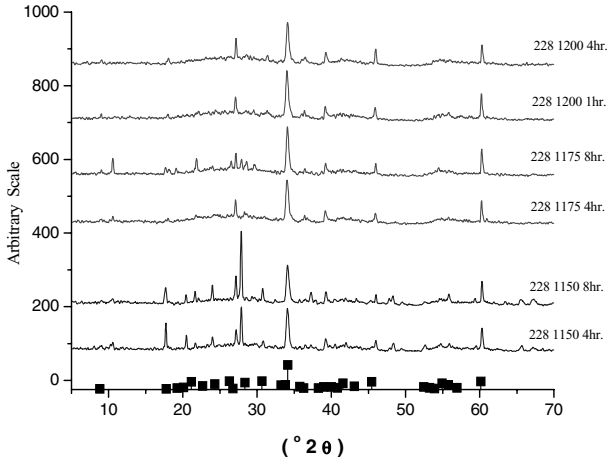


*Figure 3* The effect of increased temperature on the bulk formation of an apparent kinoshitalite phase ■, $BaMg_3Si_2Al_2O_{10}(OH)_2$, JCPDS card 43-0687) in $8SiO_2{\cdot}1.5Al_2O_3{\cdot}3.75MgO{\cdot}2.25MgF_2{\cdot}BaO$) The XRD patterns have been spaced along the $y$-axis for clarity.

glass ($y = 1.5$) a classic house of cards microstructure could be produced. This glass was therefore selected for a detailed examination of the influence of heat treatment time and temperature on microstructural development and hardness.

Fig. 3 shows X-ray diffraction patterns for the $y = 1.5$ glass heat treated to various temperatures. The crystal phase present in the bulk for all heat treatments matches that of kinoshitalite ($BaMg_3Si_2Al_2O_{10}(OH)_2$). However, it is known from MAS-NMR studies that the crystal phase is a disordered barium fluorphlogopite ($Ba_{0.5}Mg_3Si_3Al0_{10}F_2$). The amount of barium fluorphlogopite did not vary significantly with heat treatment temperature or time over the ranges studied. There are trace amounts of secondary crystal phases, notably cordierite, which is most evident in the glass heat treated at 1175°C for 8 h.

Samples heat treated below 1100°C for one hour exhibited very fine sub micron microstructures consisting of small blocky barium fluorphlogopite crystals (Fig. 4). The microstructure did not coarsen readily on increasing the crystallization hold time. The microstructure of the $y = 1.5$ glass as a function of heat

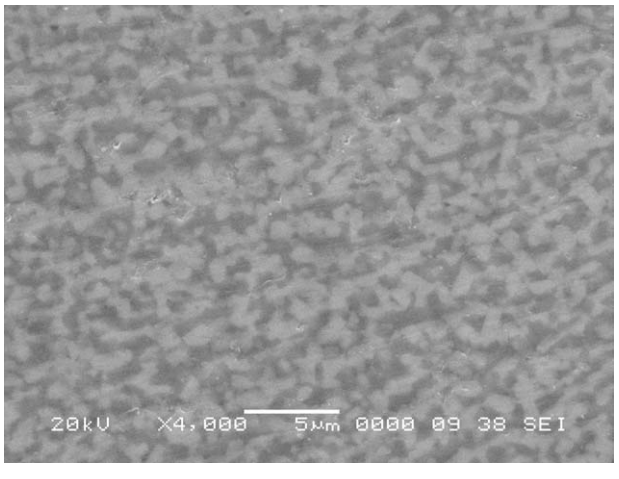


*Figure 4* Secondary Electron Image of the $y = 1.5$ glass heat treated at 655°C for one hour and 1100°C for one hour.

treatment time at 1150°C is shown in Fig. 5. The microstructure after a one hour hold at 1150°C consists of a large number of blocky barium fluorphlogopite crystals, about 1 $\mu$m in size, that are electron dense and appear white in the backscattered electron micrographs. A small number of crystals have started to exhibit an acicular morphology and are somewhat larger. The volume fraction of barium fluorphlogopite is about 0.5 and the microstructure is slightly interconnected at this stage. After a 4 h heat treatment at 1150°C the microstructure has coarsened considerably and the grains now have an appreciable aspect ratio of about four. The smallest crystals are about 4 $\mu$m in length and the largest are 15 $\mu$m in length. On increasing the heat treatment time further to 8 and 16 h there is relatively little increase in size of the barium fluorphlogopite crystals. However, some large plate-like crystals are now present and in the micrograph of the sample heat treated for 16 h there is evidence that the plates have a hexagonal structure. It must be noted that most of the crystals are plates but the chance of seeing a plate in the plane of the micrograph is very small.

Heat treatment for 1 h at 1175°C (Fig. 6) gave rise to a microstructure consisting of both small barium fluorphlogopite crystals of 1–2 $\mu$m and much larger acicular mica crystals up to 14 $\mu$m in length. On increasing the heat treatment time to 4 h the small barium fluorphlogopite crystals disappear and the microstructure consists of large acicular barium fluorphlogopite crystals that impinge on one another. The crystals are typically 8–20 $\mu$m in length and 2–4 $\mu$m in width. Increasing the crystallization hold time to 8 and 16 h had little further influence on the resulting microstructure.

Fig. 7 shows the microstructure of the sample heat treated at 1200°C for one hour. It can be seen that the interconnected house of cards microstructure has been achieved in a much shorter time than at 1150 or 1175°C (see Figs 5a and 6a respectively).

The hardness values (Fig. 8) reduce slightly on formation of the barium fluorphlogopite phase. The initial glass has a hardness value of 760 $H_v$ that falls to 625 $H_v$ for a heat treatment of one hour at 1150°C. The hardness values fall further with increasing time or increasing temperature. However, the reduction in hardness for the highest temperature studied of 1200°C is not as large as that found at 1190°C. The large reduction in hardness correlates with the formation of the interconnected house of cards microstructure.

The machinability parameters calculated from $H_v$ values, combined with imaging analysis results (i.e., area fraction) are given in Table I. The average aspect ratio ($A$) was calculated from SEM micrographs. The effective crystallinity ($Xe$), which describes crystal connectivity, would have a value of 1 if a fully connected microstructure were formed. This value is obtained from a relationship between the aspect ratio and the volume crystallinity of a sample.

Table I shows the specific cutting energy $u_1$ as a function of heat treatment temperature. The data mirrors the data for the microhardness data. There is relatively little change in specific cutting energy with heat treatment temperature for times longer than one hour. In

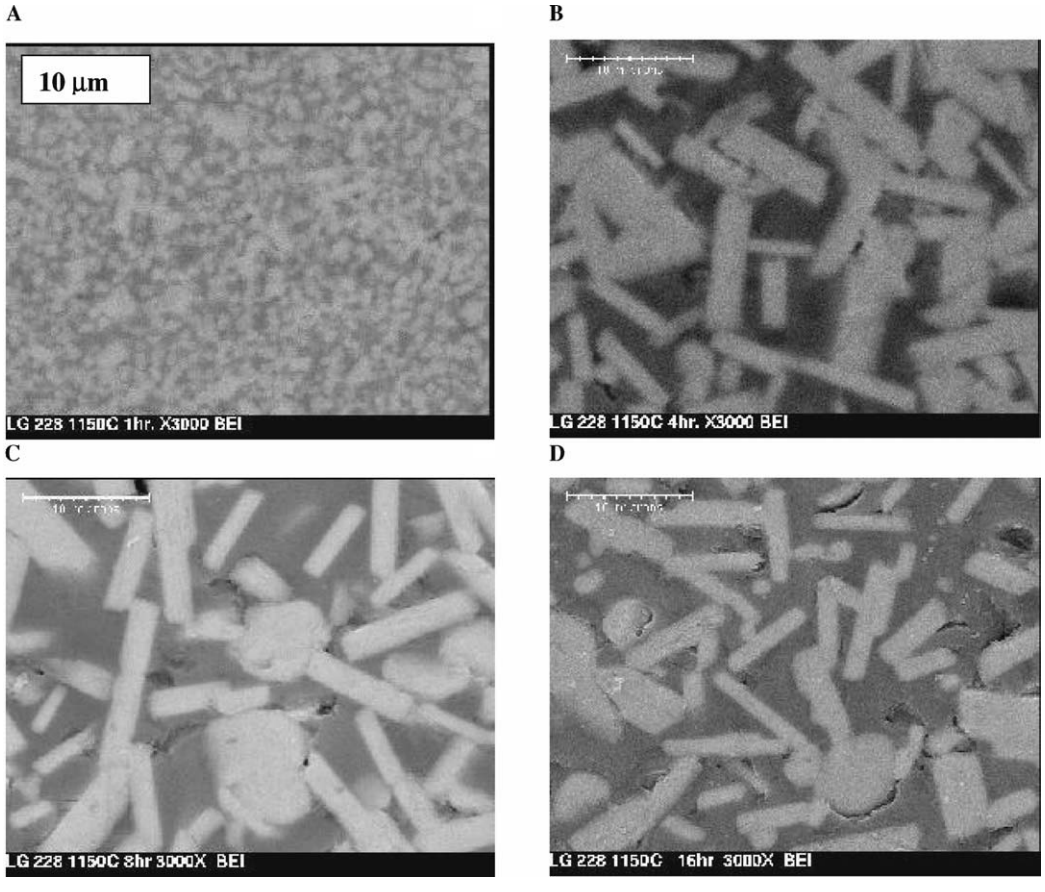


*Figure 5* Back scattered electron micrographs of the $y = 1.5$ glass heat treated for A: 1 h, B: 4 h, C: 8 h and D: 16 h at 1150°C following a one hour nucleation hold at 655°C.

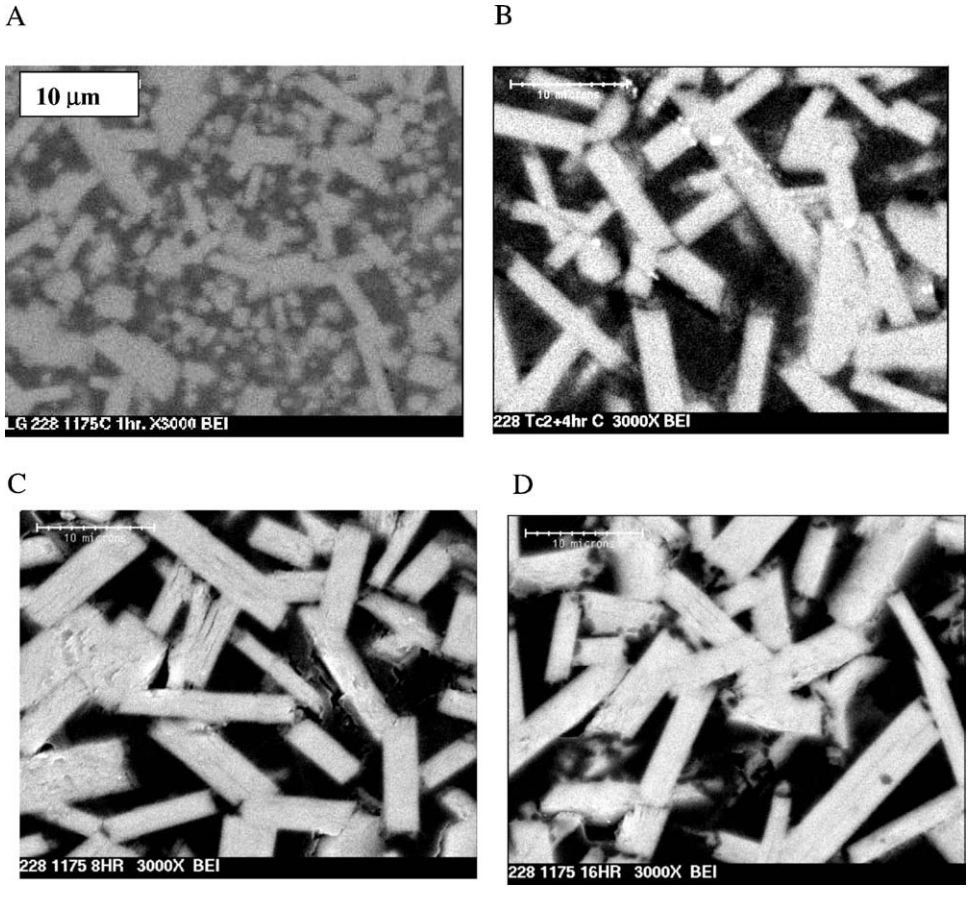


*Figure 6* Back scattered electron micrographs of the $y = 1.5$ glass heat treated for A: 1 h, B: 4 h, C: 8 h and D: 16 h at 1175°C following a one hour nucleation hold at 655°C.

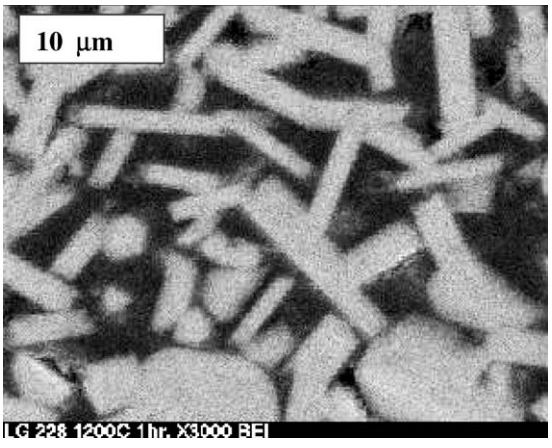


*Figure 7* Back scattered electron micrograph of the $y = 1.5$ glass heat treated for 1 h at 655°C and one hour at 1200°C.

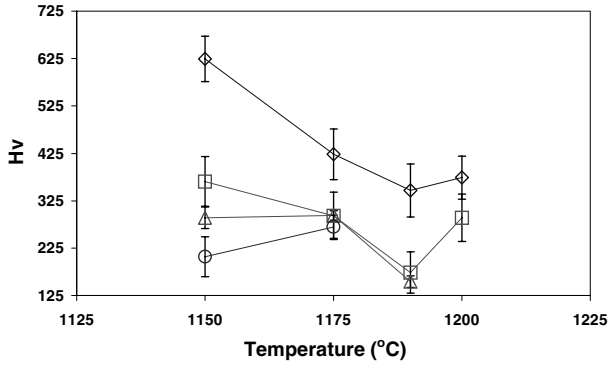


*Figure 8* Vickers microhardness ($H_v$) against temperature for $8SiO_2{\cdot}1.5Al_2O_3{\cdot}3.75MgO{\cdot}2.25MgF_2{\cdot}BaO$ (Different isothermal times are indicated by 1 h, □: 4-h, Δ: 8-h and ○: 16-h).

contrast the specific cutting energy changes markedly with heat treatment temperatures of one hour. The same phenomenon and trends are seen with the machinability data in Fig. 9. The effective crystallinity $Xe$ calculated from the micrographs is shown in Fig. 10. There is very good correlation of the effective crystallinity with the hardness, specific cutting energy and machinability plots.

TABLE I Microstructural analysis of heat-treated samples of $8SiO_2{\cdot}1.5Al_2O_3{\cdot}3.75MgO{\cdot}2.25MgF_2{\cdot}BaO$)

| Time | Heat treatment ($T_n = 655$°C) | $u_1$ (J/mm$^3$) | $n$ | $A$ | Area fraction | $Xe$ |
|---|---|---|---|---|---|---|
| 1 | 1150 | 59.02 | 0.10 | 2.09 | 0.41 | 0.25 |
| | 1175 | 24.59 | 0.14 | 3.39 | 0.48 | 0.39 |
| | 1190 | 15.69 | 0.23 | 4.95 | 0.49 | 0.50 |
| | 1200 | 18.62 | 0.20 | 4.66 | 0.53 | 0.52 |
| 4 | 1150 | 17.70 | 0.21 | 4.28 | 0.50 | 0.47 |
| | 1175 | 10.77 | 0.29 | 4.05 | 0.53 | 0.47 |
| | 1190 | 3.30 | 0.44 | 5.21 | 0.52 | 0.55 |
| | 1200 | 10.43 | 0.30 | 5.25 | 0.55 | 0.57 |
| 8 | 1150 | 10.43 | 0.30 | 4.17 | 0.52 | 0.47 |
| | 1175 | 10.85 | 0.29 | 4.45 | 0.53 | 0.50 |
| | 1190 | 2.54 | 0.46 | 4.46 | 0.55 | 0.52 |
| 16 | 1150 | 4.92 | 0.40 | 4.34 | 0.47 | 0.44 |
| | 1175 | 8.95 | 0.32 | 4.81 | 0.51 | 0.50 |

*$T_n$ describes the optimum nucleation temperature used during each heat treatment.

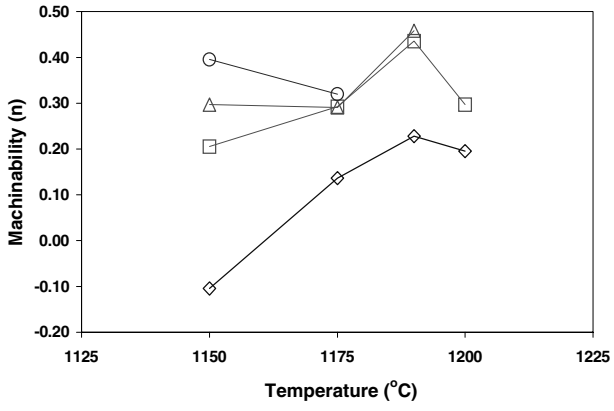


*Figure 9* Machinability, $n$, as a function of heat treatment temperature for $8SiO_2{\cdot}1.5Al_2O_3{\cdot}3.75MgO{\cdot}2.25MgF_2{\cdot}BaO$ (Different isothermal times are indicated by 1 h, □: 4-h, Δ: 8-h and ○: 16-h).

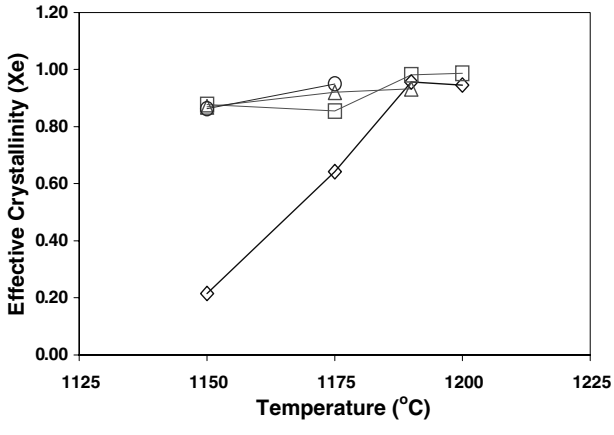


*Figure 10* Effective crystallinity, $Xe$, as a function of heat treatment temperature for $8SiO_2{\cdot}1.5Al_2O_3{\cdot}3.75MgO{\cdot}2.25MgF_2{\cdot}BaO$). (Different isothermal times are indicated by 1 h, □: 4-h, Δ: 8-h and ○: 16-h).

The optimum heat treatment (1190°C for 8-h) carried out on this $y = 1.5$ composition relate to a high effective crystallinity ($Xe$ of 0.52), a positive machinability value ($n$ of 0.46) and a low specific cutting energy value ($u_1$ of 2.54 kJ/mm$^3$). These heat treatments also illustrate the formation of crystals with a relatively low aspect ratio (approximately 5:1) resulting in a microstructure very different to that of the commercial material Macor$^{TM}$, which has an effective crystallinity of 0.82 and a higher aspect ratio (12:1). Therefore, Macor$^{TM}$ has a better interconnected microstructure than this $y = 1.5$ glass. However, this $y = 1.5$ composition should machine to higher tolerances and surface finishes because of the lower aspect ratio of its crystals. Furthermore, a lower microhardness value than Macor$^{TM}$ ($H_v$ 0.3 206) is obtained from the $y = 1.5$ glass ($H_v$ 0.3 154) with a heat treatment of 1190°C for 8-h, which is likely to indicate that an optimum microstructure has been formed. However, as this heat treatment gives rise to sample melting, and distortion during ceramming, the likelihood of this composition producing commercially useful machinable glass-ceramics without further modification is relatively low.

## 4. Conclusions

The glasses with high alumina contents gave rise to feathery microstructures that did not coarsen readily to

give blocky crystals of a high aspect ratio and therefore could not produce the classic house of cards microstructure. The glass with the lowest alumina content on heat treatment in the range 1150–1200°C gave microstructures consisting of elongated blocky crystals with a house of cards microstructure. Hardness and machinability were found to be highly dependent on the formation of an interconnected house of cards microstructure.


## Acknowledgement

The authors would like to acknowledge the financial support of the EU in the form of a Brite EuRam Contract BRPR-CT97-0521.


## References


1. T. UNO, T. KASUGA and K. NAKJIMA, *J. Amer. Ceram. Soc.* **74** (1991) 3139.
2. J. HENRY and R. G. HILL, Part I Submitted.
3. B. MILLS and A. H. REDFORD, "Machinability of Engineering Materials" (Applied Science Publishers, London, 1983).
4. D. G. GROSSMAN, *J. Amer. Ceram. Soc.* **55** (1972) 446.
5. *Idem.*, *J. Vacuum* **28**(2) (1977) 55.
6. A. G. EVANS and D. B. MARSHALL, "Wear Mechanisms in Ceramics," in Fundamentals of Friction and Wear, edited by D. A. Rigney (American Society of Metals, Ohio, 1980) p. 439.
7. G. M. ZHANG, D. T. LE and S. NG, "Assessment of Non-Linear Dynamics of Material Removal on Surface Integrity," Technical Report: University of Maryland, United States (1997).
8. D. S. BAIK, K. S. NO, J. S. CHUN and H. Y. CHO, *J. Mater. Proc. Tech.* **67** (1997) 50.
9. *Idem.*, *J. Mater. Sci.* **30** (1995) 1801.
10. A. R. BOCCACCINI, *J. Mater. Proc.* **65** (1997) 302.
11. Standard Test Methods for Microhardness of Materials, ASTMS E-384-89.



*Received 19 April 2002*
*and accepted 3 November 2003*